

Atomistic simulations of pressure-induced structural transformations in solids

R. Martoňák^a

Department of Experimental Physics, Faculty of Mathematics, Physics and Informatics, Comenius University, Mlynská dolina F2, 84248 Bratislava, Slovakia

Received 7 October 2010 / Received in final form 20 December 2010

Published online 25 January 2011 – © EDP Sciences, Società Italiana di Fisica, Springer-Verlag 2011

Abstract. Constant-pressure MD simulations complement constant-volume MD simulations and naturally allow the study of systems where external pressure is a driving force for a structural transformation. These transformations take place in crystalline as well as amorphous systems. Besides studies of bulk systems there is also growing interest in simulations of finite systems, such as clusters and nanocrystals, under pressure. In the paper we review various approaches to constant pressure simulations with focus on the recent developments in simulation methodology, such as metadynamics and transition path sampling. The application of the techniques to bulk and finite systems is illustrated on several examples.

1 Introduction

External pressure controls the volume of the physical system and therefore is one of the most important parameters determining short- and long-range order and resulting structural and other properties of condensed matter systems. While generally an increase of pressure results in continuous compression of the system, at certain values a discontinuous change of properties may occur. In crystals this is usually associated with change of arrangement of the structural units, atoms or molecules, and typically implies a change of symmetry of the lattice. Different microscopic arrangement and lattice symmetry may result in pronounced differences in macroscopic physical and chemical properties. If the symmetry groups of the two structures are not in a group-subgroup relation, according to the Landau theory of phase transitions such structural transformation represents a first-order phase transition. The existence of a given substance in different crystalline forms has been known since long time and is known as *polymorphism*. Pressure is one of key variables that can be used to control polymorphism and pressure-induced phase transitions can be employed to prepare new structures.

Except for phase boundaries, at given external conditions such as pressure and temperature only one crystalline phase is thermodynamically stable. However, a transformation from one crystal structure to another might require a non-trivial reorganization of the atoms or molecules as well as their chemical bonds. Clearly, in a dense solid phase this may be associated with a high free-energy barrier between the phases. The difficulty of transforming from one structure to another often causes pronounced *metastability* beyond the thermo-

dynamic stability region and e.g. at ambient conditions one can observe the simultaneous existence of several crystalline phases. A well-known example is graphite and diamond, which have remarkably different properties. At ambient conditions the diamond phase is metastable and only graphite should exist; however, due to strong covalent bonds a spontaneous conversion of diamond to graphite is practically not observed.

The existence of polymorphism raises a number of challenges for theory. The fundamental one is to predict the stable polymorph at given pressure P and temperature T , knowing the chemical composition of the system. This is known in literature as the crystal structure prediction problem (CSP). Clearly, solution of the CSP would allow the calculation of phase diagram for any given substance and prediction of the properties of different phases even prior to their synthesis, which would have a large impact in number of fields of science and technology. Apart from predicting the stable polymorph it might be of importance to predict also metastable polymorphs. Thermodynamics offers in principle a simple approach to the solution of CSP from scratch, since stable and metastable crystal structures represent global or low-lying local minima of the Gibbs free energy $G = U + PV - TS$, where U is the internal energy of the system, P the external pressure, V is volume of the system, T is temperature and S is entropy. Since the calculation of entropy is well known to be difficult, it is often neglected and instead of the Gibbs free energy one minimizes the enthalpy, which effectively corresponds to the $T = 0$ case. Under this simplification standard optimization algorithms such as e.g. simulated annealing [1] can be applied. A remarkable success has been achieved in recent years due to application of evolutionary algorithms [2] and simple random search methods [3].

^a e-mail: martonak@fmph.uniba.sk

Beyond the location of the phase boundary, however, thermodynamics does not provide any information about the mechanism of the transition. Study of structural transformations offers an alternative route to the solution of the CSP. Provided at least one initial structure is known, inducing structural transformations by changing external parameters can be used to find new phases. The advantage of such finite-temperature approach is that entropic effects are taken into account and phases dynamically stabilized by entropy can be found, too. Prediction of crystal structures is, however, not the only motivation here. Other important aspects are the study of the driving force of structural transformations and understanding of the detailed microscopic mechanisms. The knowledge of the mechanism, apart from intrinsic theoretical interest, can help to suggest experimental protocols able to drive the system towards the desired transition. Experimentally, the determination of the pathways followed by individual atoms in course of a structural transformation of a crystal is at present extremely difficult, if not impossible.

The theoretical and practical importance of studying polymorphism is broad. In Nature there are systems where matter is under high pressure and/or temperature, such as e.g. the interiors of the Earth and of other planets. Understanding of structural behaviour of solid systems under such extreme conditions is crucial for the study of the relevant physics. Another field of application is materials science where pressure may stabilize non-standard bonding patterns and thus can be used as a tool for preparation of new materials with specific or unusual properties (e.g. preparation of superhard materials [4] by application of high pressure). Polymorphism is also very important in chemical and pharmaceutical industry where the crystallization process in fabrication is controlled by kinetic factors. The resulting product may therefore not always correspond to the thermodynamically most stable form [5] and if a wrong polymorph is produced the product may fail to exhibit the desired properties.

Principal route to study structural transitions in solids is experimental and pressure is very often used as a main tool to prepare new phases. Both dynamic and static compression techniques are widely used [6]. The major achievement was the progress in the diamond anvil cell techniques which allow to reach pressures in the megabar region (for comparison, pressure in the Earth's inner core reaches ~ 3.6 Mbar). In combination with modern synchrotron light sources and neutron facilities it allows the diffraction studies and other experimental probes, such as various spectroscopies, to be performed in situ (see Ref. [6] and references therein). Recently due to progress in ramp-wave compression techniques it became possible to study solids at peak pressures reaching beyond 10 Mbar [7].

A complementary approach is provided by computer simulations. Due to impressive progress in *ab initio* techniques and computer hardware these have nowadays reached the level of accuracy and reliability which allows them in many cases to predict the outcome of real experiment. As such they can be used as substitution

for the latter, which is particularly important when performing the real experiment is either too complicated or expensive, or simply impossible. This is precisely the case in study of materials under extreme conditions such as pressure and temperature, where terrestrial experiments easily reach their intrinsic limits. On the other hand, using the computer as "virtual laboratory", experiments can be performed at relatively low cost.

Computer simulation of structural transitions in crystals is, however, not an easy task. Such phase transitions are often of first order and proceed via nucleation and growth, involving crossing an activation barrier. Even in Nature these often proceed on long time scales, which may exceed by many orders of magnitude those currently accessible to computer simulations. This generic problem is well-known in simulations as the "time-scale gap problem". While the standard simulation algorithm, Parrinello-Rahman variable-cell constant-pressure molecular dynamics [8] and its variants (see Sect. 2) have been successful in many cases, there is a number of transitions and phases that could not be observed in this way. This points to the need for further methodological development. Some years ago a new approach to this problem was developed [9], based on the general metadynamics algorithm [10]. This effectively cures the time-scale problem by introducing an intrinsic mechanism for barrier crossing and overcomes many of the difficulties of the previous approaches. It has been successfully applied to a number of inorganic and organic crystals and opens a way to study complex reconstructive structural transformations, including those which proceed via a number of intermediate states. Another powerful approach to the study of structural transformations is the application of the transition path sampling method [11], which has been successfully applied to several materials [12–14].

Besides crystalline solids, however, there are also amorphous ones, and some of them represent materials of great practical importance (e.g. silica glass). An interesting question is how does this class of materials respond to increasing pressure and whether there is some analogue of polymorphism. Perhaps surprisingly, the answer, at least in some systems, appears to be positive. Although amorphous systems are isotropic and lack long-range order and therefore pressure cannot induce a change of symmetry, it can still induce pronounced changes in the local and medium-range order as well as in density. In some cases these changes appear to have discontinuous character and are similar to phase transitions. The existence of two or more amorphous forms of the same substance is called *polyamorphism*. Study of polyamorphism currently represents a very interesting and promising direction in study of structure of condensed matter. Polyamorphism is as yet not fully understood and the interest here is both fundamental and practical. On the fundamental side, this exciting phenomenon shows that the spectrum of states of condensed matter is likely to be considerably broader than traditionally assumed. Since polyamorphism also offers a practical possibility of creation of new materials, studies in this field including computer simulations are of interest also for materials science.

In the above considerations we had in mind bulk crystalline or amorphous systems. Structural transformations, however, are not limited to bulk systems. In the last two decades it became possible to experimentally prepare small nanoscale objects such as nanocrystals in a controlled way and investigate their properties under pressure. Besides being interesting for nanotechnology, such studies are highly interesting for purely theoretical reasons. Since nanocrystals can be regarded as “interpolation” between molecules and bulk systems, studying the size dependence of structural transitions can provide valuable information about the respective mechanisms, in particular when the size of the system becomes comparable to the size of the nucleation region. It is clearly desirable to complement also this kind of experiments by simulations. The standard methods for simulations of pressure-induced phase transitions were, however, designed for bulk systems and as such are not directly applicable to the study of finite objects under pressure. In order to fill this gap a number of techniques were developed which enable simulation of finite objects under external pressure [15–17].

In the present paper we review the above mentioned theoretical developments. In Section 2 we discuss constant-pressure MD as basic approach to simulations of structural transitions in solids. In Sections 3 and 4 we review applications of more advanced approaches, such as metadynamics and transition path sampling, to simulations of structural phase transitions in crystals. In Section 5 we briefly mention simulations of polyamorphism, using water as example. In Section 6 we discuss simulations of finite objects under pressure. Finally, in the last Section 7 we draw some conclusions and discuss possible directions of future developments.

2 Constant-pressure molecular dynamics simulations

As mentioned in the introductory section, a possible route to find crystalline phases is provided by simulation of structural phase transitions. Compared to the thermodynamics-based optimization methods the advantage of this approach is that it can yield also information about transformation mechanisms. Starting from an initial crystal structure one can follow the evolution of the system upon change of external parameters, such as pressure.

Straightforward constant-volume MD simulations that are commonly used in simulations of liquids, are, however, not suitable for simulation of solid-solid structural transitions. The first reason is that it is preferable to control pressure rather than volume. More important, however, is the fact that the use of periodic boundary conditions (common in simulations) implies that the supercell must be commensurate with the unit cell of the crystal. In other words, the supercell size along each edge direction must contain an integer number of unit cells of the crystal. In course of a structural transition, however, the unit cell changes and if the supercell was chosen to be appropriate for the initial structure, it is unlikely to be so for the final

one. The resulting mismatch will introduce a free energy penalty that is likely to prevent the observation of the transition.

The first constant-pressure MD method was developed by Andersen [18]. Constant-pressure conditions were maintained by means of isotropic volume scaling that was automatically performed during the simulation according to the difference between the instantaneous microscopic pressure and prescribed external hydrostatic pressure. Technically this was achieved by means of introducing an extended Lagrangian which coupled the dynamics of the particles with dynamics of the volume under the condition of constant pressure. We note here that this conceptually very important idea was later used in several other simulation schemes (Hoover [19], Parrinello-Rahman [8], Car-Parrinello [20], etc.). The method of Andersen generates isoenthalpic-isobaric (N, P, H) ensemble and allowed constant-pressure simulation of liquids. We will not discuss technical details here and proceed directly to its generalization for solids due to Parrinello and Rahman [8,21].

The method of Andersen allowed only the volume of the box to fluctuate, but not its shape. Therefore it was not suitable for simulations of crystals and in particular it could not be applied to the simulation of structural phase transitions where besides the volume also the box shape has to adapt to the unit cell of the new structure. It is convenient to arrange the three edge vectors $\mathbf{a}, \mathbf{b}, \mathbf{c}$ of the supercell as a 3×3 matrix $\mathbf{h} = (\mathbf{a}, \mathbf{b}, \mathbf{c})$. The scheme of Parrinello and Rahman [8] (PR) treats all elements of the general box matrix \mathbf{h} as dynamical variables. Scaled particle vectors \mathbf{s}_i are introduced via $\mathbf{r}_i = \mathbf{h}\mathbf{s}_i$; the distance between particles i and j is given by $r_{ij}^2 = (\mathbf{s}_i - \mathbf{s}_j)^T \mathbf{G} (\mathbf{s}_i - \mathbf{s}_j)$ where $\mathbf{G} = \mathbf{h}^T \mathbf{h}$ is the metric tensor. It is also useful to define a matrix $\boldsymbol{\sigma} = V \mathbf{h}^T \mathbf{h}^{-1}$ where $V = \det \mathbf{h}$ is the volume of the supercell. The extended Lagrangian is defined as

$$\mathcal{L} = \frac{1}{2} \sum_i m_i \dot{\mathbf{s}}_i^T \mathbf{G} \dot{\mathbf{s}}_i - \sum_{i < j} u(r_{ij}) + \frac{1}{2} W \text{Tr} \dot{\mathbf{h}}^T \dot{\mathbf{h}} - PV, \quad (1)$$

where W is a fictitious mass. For simplicity a pair potential was assumed here. From \mathcal{L} one derives the equations of motion for the scaled variables \mathbf{s}_i and box \mathbf{h}

$$\begin{aligned} m_i \ddot{\mathbf{s}}_i &= - \sum_{j \neq i} \frac{u'(r_{ij})}{r_{ij}} (\mathbf{s}_i - \mathbf{s}_j) - m_i \mathbf{G}^{-1} \dot{\mathbf{G}} \dot{\mathbf{s}}_i \\ W \ddot{\mathbf{h}} &= (\boldsymbol{\pi} - P) \boldsymbol{\sigma}, \end{aligned} \quad (2)$$

where

$$\boldsymbol{\pi} = \frac{1}{V} \left(\sum_i m_i \mathbf{v}_i \mathbf{v}_i - \sum_{i < j} \frac{u'(r_{ij})}{r_{ij}} \mathbf{r}_{ij} \mathbf{r}_{ij} \right) \quad (3)$$

is the internal pressure tensor of the system and $\mathbf{v}_i = \dot{\mathbf{h}} \mathbf{s}_i$. It was shown that this dynamics generates the isoenthalpic-isobaric (N, P, H) ensemble. The scheme naturally allows for structural transformations: if the

atomic configuration undergoes a change and the system within the current box is not anymore in equilibrium at prescribed external pressure, the supercell will gradually adapt to the new configuration until a new dynamical equilibrium is reached. We note that the scheme was also generalized from hydrostatic pressure P to the case of general anisotropic constant stress \mathbf{S} [21]; therefore it also allowed a simulation of system under conditions of uniaxial tension or compression, shear load, etc. The artificial mass W determines the time scale of the volume fluctuations and its value is irrelevant for the static averages calculated along the trajectory. However, it is convenient to choose its value in such way that the time scale of the volume fluctuations is approximately equal to L/c where L is the box size and c is the sound velocity in the bulk system.

Without intending to provide an exhaustive historical overview we briefly review here several further developments of the constant-pressure MD schemes after the seminal works of Andersen and Parrinello and Rahman. Nosé and Klein [22] discussed various technical aspects of the application of both methods to molecular systems, including the conservation laws, choice of the artificial mass and use of symmetric box matrix \mathbf{h} to avoid rotations of the box. While both methods generate the constant enthalpy (N, P, H) ensemble, in simulations it is usually more practical to control temperature rather than enthalpy. Already in the original paper [18], the constant-pressure scheme was complemented by stochastic forces changing the kinetic energy of the atoms (stochastic collisions). A more practical solution was suggested by Nosé [23] who used the extended Lagrangian idea and showed that by introducing additional variable which scales time, it is possible to generate isothermal (canonical) ensemble from deterministic equations of motion. Hoover showed that the Nosé method could be reformulated to a more convenient form, avoiding the scaling of time [19] by introducing additional terms corresponding to friction. The resulting equations of motion, however, did not generate the exact (N, P, T) ensemble. Later, Melchionna et al. [24] modified the Hoover equations to sample the proper (N, P, T) ensemble and extended the scheme to use of multiple thermostats as well as to constrained dynamics, allowing simulation of molecular systems. Wentzcovich [25] pointed out that the kinetic energy term in the Parrinello-Rahman Lagrangian depends on the choice of the vectors of the box matrix \mathbf{h} (which is, in principle, arbitrary) and therefore does not satisfy the requirement of modular invariance. An alternative version of variable-cell MD was also proposed in reference [25]. Martyna et al. [26] formulated modularly invariant versions of isothermal-isobaric MD allowing isotropic and anisotropic volume fluctuations, as well as a hybrid scheme where two different time scales were associated with the two different kinds of cell fluctuations. The condition of constant temperature was maintained by using Nosé-Hoover chain thermostats [27]. Schemes which use directly the metric tensor \mathbf{G} as dynamical variable, rather than the box \mathbf{h} , have also been developed [28]. Besides extended Lagrangian schemes there is also a different approach due to Berendsen et al. [29] where temperature

and pressure are controlled by rescaling of velocities and coordinates (together with supercell vectors), respectively, according to the instantaneous deviation of temperature and pressure from their prescribed values. While this approach itself does not correctly sample the (N, P, T) ensemble it is often used in the equilibration phase where it is very efficient since it does not lead to oscillatory behaviour even if the initial state of the system is far from equilibrium. Recently a new temperature-control scheme was developed [30] which extends the Berendsen thermostat by including a stochastic force. This approach samples the canonical ensemble and has been also combined with barostat [31] to sample the (N, P, T) ensemble. The PR method and its variants became standard tool for studies of structural transitions. Particularly after the generalization to ab initio simulations [32] it acquired a predictive value and has been used in many cases (see paper [33] and references therein).

The PR method and its above-mentioned generalizations, however, share the limitations common to all standard MD methods, in particular the time-scale gap problem. In case of solid-solid structural transitions this may become particularly severe. In experiment, first-order phase transitions proceed by heterogeneous nucleation which is likely to initiate at surface or extended defects, such as dislocations. Because of the periodic boundary conditions and small size of the supercell, there is no surface and no extended defects and therefore the heterogeneous nucleation is essentially suppressed. This forces the structural transition to proceed via some kind of collective mechanism, resulting in a large barrier. Clearly, the large barrier aggravates the time-scale problem, making the spontaneous observation of a transition at equilibrium conditions practically impossible. The situation is shown in Figure 1.

The simplest solution is to increase the pressure. If there is a substantial difference in the volume of the two phases, with increasing pressure the Gibbs free energy of the initial phase with larger volume increases with respect to that of the final phase with smaller volume. Consequently, the barrier also lowers and at some external pressure value p' the barrier vanishes. At that point the system has reached the limit of mechanical stability and the initial phase cannot anymore exist as a stable phase (Fig. 1). The transition starts immediately and usually is well observable on the time scale of several ps which can be easily followed also in ab initio simulations. The problem is, however, that the overpressurization is often quite substantial and p' may be larger than p_{eq} by an order of magnitude or more. Clearly, the kinetics of the transition observed in this way may not be realistic. Moreover, overpressurization severely affects the predictive value of the method, since it may cause some phases to be skipped, especially in case of a complex phase diagram where some phases are stable only in narrow pressure interval. Finally, if there is little volume difference between the phases, overpressurization is of little help. The origin of the problem is clear: standard MD does not possess any mechanism that would accelerate the crossing of high barriers and it is not possible to follow the dynamical evolution of the system

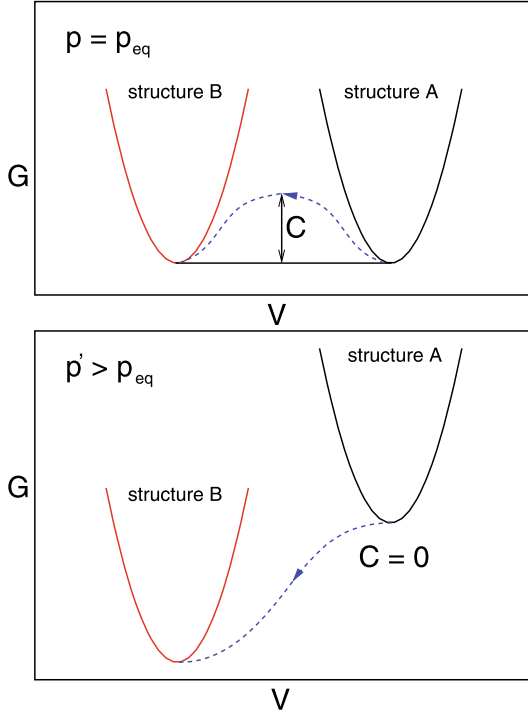


Fig. 1. Upper panel: first order transition at equilibrium pressure p_{eq} where the Gibbs free energies of the two phases A and B are equal. The phases are separated by a large barrier C . Lower panel: first order transition at pressure $p' > p_{eq}$ where the barrier C vanishes and the system reaches the point of mechanical instability.

over time long enough to observe the transition to occur spontaneously. A more realistic approach to the simulation of solid-solid phase transitions thus has to address the problem of crossing the barrier.

3 Simulations of structural transitions in crystals by the metadynamics algorithm

In physics, chemistry and other fields one often encounters activated processes, where the system moving on the free-energy landscape between two minima A and B has to overcome a barrier C . If $C \gg k_B T$, such process is a rare event and its spontaneous observation on time scales reachable in MD simulations is practically impossible. Well-known examples are e.g. chemical reactions, first-order phase transitions and protein folding.

Several methods have been proposed in order to treat this problem and accelerate the escape of the system from the basin of attraction of the initial minimum [34–36]. In this paper we concentrate on the class of methods based on application of a suitably constructed artificial biasing potential. This aims at lowering the barrier and facilitates its crossing. In conformational flooding [35] the biasing potential is applied in the form of a Gaussian function in the configuration space based on estimated shape of the free energy well around the minimum. The estimate can be calculated by performing a short MD simulation. In

the local elevation method [36] the biasing potential in the configuration space is instead constructed iteratively as sum of Gaussians.

In reference [10] Laio and Parrinello proposed a new technique called metadynamics which proved to be efficient and easy to implement. The important step here is a dimensionality reduction. Instead of studying the problem in the full $3N$ dimensional configuration space (N is the number of particles), it is often possible to identify a relatively small number of collective coordinates $(s_1, \dots, s_m) = \mathbf{s}$, which provide a coarse-grained description of the system and are able to distinguish between the different free energy minima. These collective variables may characterize, e.g., some geometrical properties of the system such as bond lengths or angles, coordination numbers, etc., and are often called order parameters. It is useful to include in the space of collective variables the slow degrees of freedom of the system. In such case, if one forces the system to stay close to a given point in the space of the collective variables, it is easily possible to equilibrate the remaining (fast) degrees of freedom by a relatively short MD simulation. In general case, if the collective variable \mathbf{s} is a function of the atomic coordinates, one can enforce a certain value of \mathbf{s} e.g. by means of Lagrange multipliers and this technique provides also an information about the free-energy derivatives $\frac{\partial \mathcal{F}(\mathbf{s})}{\partial \mathbf{s}}$ (see Refs. [37,38]).

Metadynamics is an algorithm which allows to explore the free energy surface $\mathcal{F}(\mathbf{s})$ and find low-energy pathways connecting the adjacent minima across the barriers. Its original formulation [10] is based on a discrete dynamics

$$\mathbf{s}^{t+1} = \mathbf{s}^t + \delta s \frac{\phi^t}{|\phi^t|} \quad (4)$$

of steepest-descent type where each step, following the direction of the normalized force $\frac{\phi^t}{|\phi^t|}$, moves in the collective-variable space over a fixed distance δs . The force ϕ^t

$$\phi^t = -\frac{\partial \mathcal{F}^t(\mathbf{s})}{\partial \mathbf{s}} \quad (5)$$

is derived from a modified free energy $\mathcal{F}^t(\mathbf{s})$ where a history-dependent term has been added to $\mathcal{F}(\mathbf{s})$

$$\mathcal{F}^t(\mathbf{s}) = \mathcal{F}(\mathbf{s}) + \sum_{t' < t} W e^{-\frac{|\mathbf{s} - \mathbf{s}^{t'}|^2}{2\delta s^2}}. \quad (6)$$

The history-dependent term is constructed as sum of Gaussians placed at each previously visited point in the \mathbf{s} -space. The Gaussians act as biasing potential and tend to discourage the dynamics (4) from visiting again the same point. The resulting dynamics is non-Markovian, since it depends on the history. In this way, the total biasing potential is constructed iteratively, step by step. As the dynamics proceeds, the initial free-energy well is gradually filled with Gaussians and when the transition state is reached, the system enters into the basin of attraction of a new minimum.

We note that the scheme does not require the calculation of the free energy $\mathcal{F}(\mathbf{s})$ itself; instead only its derivatives $\frac{\partial \mathcal{F}(\mathbf{s})}{\partial \mathbf{s}}$, which are considerably easier to calculate, are needed. Besides the ability to escape free-energy minima the technique is under certain conditions also able to recover the free energy landscape $\mathcal{F}(\mathbf{s})$. Provided the evolution of the system at every metastep is reversible, in the long-time limit the modified free energy approximately tends to a constant $\lim_{t \rightarrow \infty} \mathcal{F}^t(\mathbf{s}) \rightarrow \text{const}$ within the explored region of the collective variable space. The sum of the Gaussians therefore converges to a mirror image $-\mathcal{F}(\mathbf{s})$ of the underlying free energy, up to an additive constant. In this sense metadynamics can be seen as a method performing iterative approximate coarse-grained integration of the free energy in the multi-dimensional space of the collective variables. If the evolution of the system is not perfectly reversible, it might not be possible to extract the free energy landscape $\mathcal{F}(\mathbf{s})$ from metadynamics simulation. However, the algorithm can still be used to search for low-energy pathways leading to new minima, starting from an initial one. More information about metadynamics algorithm and its various variants and applications can be found in review papers [39,40].

In order to eliminate some of the difficulties of the PR method discussed in Section 2, in reference [9] the metadynamics approach was applied to the simulation of structural transitions. The most important point in the implementation of the general metadynamics algorithm is the choice of the collective variables. In case of crystals, the structure is defined by the unit cell and set of fractional coordinates of the atoms. As discussed at the beginning of this section, the unit cell is related to the supercell and therefore a natural choice is to take the supercell box matrix \mathbf{h} as collective variable, or order parameter. This can distinguish different crystal structures, similarly to the PR method (more detailed discussion of the relation between supercell and unit cell can be found in the review paper [33]). In reference [9] an algorithm based on these ideas was developed, where metadynamics is applied to the free energy surface $G(\mathbf{h})$ representing the Gibbs free energy expressed as a function of the \mathbf{h} matrix. Technically the implementation of metadynamics in this case is easy since the box matrix \mathbf{h} is an independent variable which does not depend on atomic coordinates and therefore its value is directly imposed on the system. Moreover, a change of the simulation cell represents a deformation and the derivative of the free energy with respect to strain components can be obtained from the stress tensor. The evaluation of the derivative $\frac{\partial G(\mathbf{h})}{\partial h_{ij}}$ is therefore very simple [9,33,42]

$$\frac{\partial G}{\partial h_{ij}} = V [\mathbf{h}^{-1}(\boldsymbol{\sigma} + P)]_{ji} \quad (7)$$

and requires only the evaluation of the average stress tensor $\boldsymbol{\sigma}$ (here we follow the standard sign convention for the stress tensor where hydrostatic pressure P is represented as $\sigma_{ij} = -P\delta_{ij}$). This can be easily performed in a short (~ 1 ps) constant volume and constant temperature MD simulation. Filling of the free energy well corresponds to

the exploration of the space of possible deformations of the crystal. Different deformations, including all kinds of volume and shear deformations, are gradually applied in the order of increasing Gibbs free energy, until a structural transition occurs. We note that in order to eliminate three degrees of freedom related to global rotations of the supercell it is convenient to assume a special form of the box matrix \mathbf{h} , such as symmetric [9] of upper triangular [33]. This reduces the dimensionality of the order parameter from 9 (3×3 matrix \mathbf{h}) down to 6.

One of the advantages of this approach is that it is very easy to implement. It can be combined with MD (and also Monte Carlo or Langevin dynamics etc.) simulation using classical (force field) or quantum (ab initio or tight binding) description of the system. There is no need to modify existing MD codes and the algorithm can be coded in the form of a driver which calls the MD code and reads from its output file the average stress tensor (see Figs. 1 in Refs. [33,41] for a flow chart of the algorithm). Early applications to benzene [42] and zeolite [43] were performed using classical potentials while in later studies ab initio metadynamics was applied to the study of the perovskite to post-perovskite transition in MgSiO_3 [44] and phases of phosphorus [45]. An alternative continuous version of the algorithm has also been formulated in reference [46].

In references [47,48] an improved version of the algorithm was proposed. The Gibbs free energy $G(\mathbf{h})$ is along certain directions likely to be a quite steep function of the components of the matrix \mathbf{h} . This is partly due to the anisotropy of the crystal, and mainly due to the coupling between components of \mathbf{h} . The latter is easily understood considering the difference between volume-conserving and volume-nonconserving deformations. If a crystal is compressed along all axes, the volume is compressed, too, and the energy cost of such deformation is usually much higher than that of a deformation where compression along one axis is compensated by expansion in a perpendicular direction, without changing the volume. The basin of attraction of a crystal structure thus may have very different curvature in different directions, and is likely to be narrow in the direction of volume gradient and broad in perpendicular directions. Clearly, spherical Gaussians are not optimal for filling, since they need to be small with respect to the narrow direction in order to guarantee that the filling proceeds regularly and the escape occurs via lowest energy path. Small Gaussians, however, result in a large number of metasteps needed to reach the transition state, which is impractical. If the Gaussians are too large, the system may escape in essentially random direction and in a system with complex free energy landscape e.g. an amorphization could occur instead of a transformation to another crystal structure.

The improved technique presented in references [47,48] introduced instead of the box matrix \mathbf{h} new scaled coordinates (preconditioning) which take into account the shape of the initial free energy well and guarantee that all kinds of deformations are treated on equal footing (for technical details we refer to Refs. [41,47–49]). This improvement was shown to be important in study of

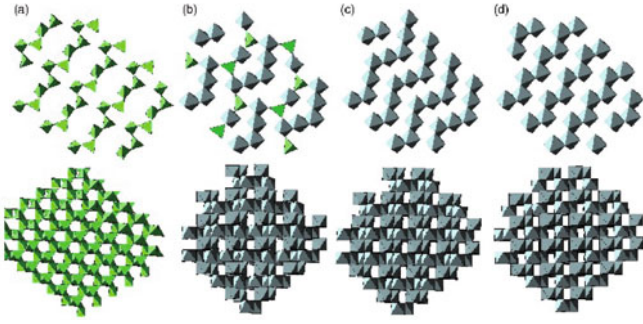


Fig. 2. Section of a $(11\bar{2})$ plane (top row) and side view (bottom row) of the metastable structures encountered in the transition from cristobalite-XI (a) to the α -PbO₂-like phase of silica (d). The transition occurs via the formation of a mixed tetrahedral and octahedral structure (b) and of a defective octahedral structure made of alternating 2×2 and 3×3 planes (c). After reference [51].

pressure-induced phase transitions in silica starting from α -quartz and coesite [47,48]. Afterwards the technique was successfully applied to a number of systems, such as post-diamond phases of carbon [50], silica starting from α -cristobalite [51], silicon [52,53], carbon dioxide [54], calcium [55], MgSiO₃ [56,57] and CdSe [58]. A recent detailed review of the method and its applications can be found in the book chapter [49].

For illustration we mention here two of the above examples. First we show a simulation of pressure-induced transitions starting from the α -cristobalite polymorph of silica. In this system strong kinetic effects are observed in experiment [59,60], resulting in an anomalous sequence of phases. When α -cristobalite is compressed at room temperature to 370–450 kbar, it should transform to stishovite, which is the stable phase in this pressure range. Instead, however, a transformation to the α -PbO₂-like phase is observed, which is at these conditions a metastable phase. In reference [51] this transformation was studied by ab initio metadynamics and both transition to stishovite and to the α -PbO₂ phase were found. In Figure 2 the evolution of the system in course of the transition to the α -PbO₂ phase is shown. It is seen that the transformation proceeds in several steps and passes via intermediate states. In reference [51] the barriers separating the initial and first intermediate state were calculated for both observed pathways and it was found that the one leading to the α -PbO₂ phase has a lower barrier, which is compatible with experiment. We note that in reference [51] the method was generalized also to the case of general non-hydrostatic external stress.

Second example is simulation of pressure-induced polymerization of carbon dioxide. While forming a molecular solid at low temperatures and pressures, CO₂ at high pressure can form a polymeric covalent network, and intuitively one can expect a formation of tetrahedral phases similar to those known in SiO₂. Polymerization of CO₂ was studied by ab initio metadynamics in reference [54] and one of the results was a prediction of transformation of molecular phase III into polymeric structure $P_{41}2_12$.

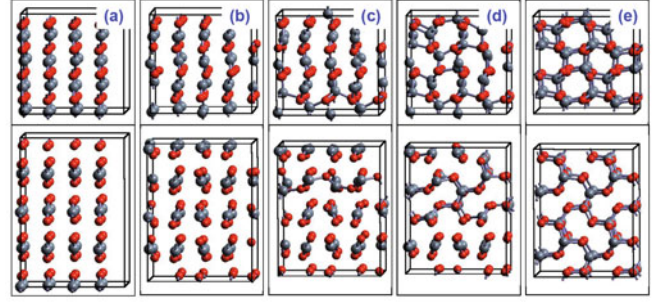


Fig. 3. Illustration of the intermediate structures (metastep 1, 14, 16, 17, 100) during the transformation of CO₂ from phase III ($Cmca$) to the α -cristobalite-like phase ($P_{41}2_12$) at 80 GPa and 300 K, where upper frames are top views and lower frames are side views. The density increases from 3.63 to 4.23 g/cm³ from metastep 1 to metastep 100. After reference [54].

This structure is actually similar to the α -cristobalite polymorph of silica and is predicted to be created at temperatures below the room temperature. At higher temperature defects are created and ultimately the pressure-induced transformation results in amorphous phase, consistent with experiments [61,62]. This illustrates that in simulations it is possible to take into account the effect of temperature on structural phase transitions.

To conclude this section we note that the box matrix \mathbf{h} represents a global collective variable which affects the whole simulated system. Therefore, when used as order parameter, it might to some extent favour a collective mechanism of the transition. This is more likely to occur when the system size is small, typically in ab initio metadynamics where the system size is rather limited. In such case the transformation mechanism observed in the metadynamics simulation is more likely to represent what happens inside the nucleation region rather than proper nucleation and growth process where the new phase gradually propagates inside the initial one.

4 Simulations of structural transitions in crystals by transition path sampling

Another generic and powerful simulation technique that has been applied to simulations of structural phase transitions in crystals is transition path sampling (TPS) [11]. This approach was developed for simulation of rare events and in combination with constant-pressure MD is well suited for study of structural phase transitions in crystals. TPS is based on Monte Carlo importance sampling of the space of dynamical trajectories connecting the initial and final states which need to be characterized by distinct values of a suitably chosen order parameter. The sampling is performed by repeated propagation of the system forward and backward in time and slightly modifying the atomic velocities (for details see the original paper Ref. [11]). One can start from an initial guess for the trajectory and in course of the sampling process the dynamical trajectory converges towards the favored mechanism (analogue of

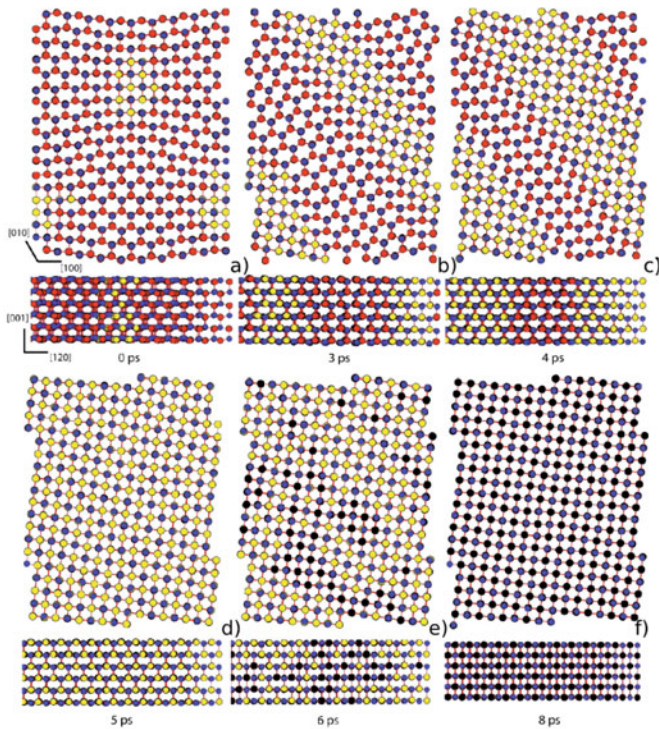


Fig. 4. B4 (Wurtzite) to B1 (Rocksalt) phase transition in GaN. The figure shows snapshots from a representative trajectory harvested in TPS MD. The colors reflect the coordination number (CN) of Ga atoms: CN = 4 red, CN = 5 yellow, CN = 6 black. The formation of an intermediate (d) on the route to B1 (f), following nucleation (a) and growth (b-c) steps are clearly observed. Adapted from reference [63].

equilibration in ordinary MD or MC simulation). TPS is able to study nucleation and growth processes in first-order structural transitions and avoids overpressurization typical of plain constant-pressure MD. The technique has been applied to several bulk systems [12–14,63] (for applications of TPS to finite systems see Sect. 6). An example of application of TPS to a study of the B4 \rightarrow B1 transition in GaN is shown in Figure 4 (for details, see Ref. [63]).

5 Simulations of polyamorphism

As mentioned in the introduction, even in non-crystalline disordered solids pressure can bring about profound changes taking place in apparently discontinuous manner. Although in some cases it is not yet firmly established whether these structural transformations represent genuine first-order phase transitions, the change of structure upon change of pressure can be quite sharp. Examples of this polyamorphism include e.g. well-known tetrahedrally bonded systems, such as Si, Ge, SiO₂, H₂O, but also S and other systems. A particularly interesting case is water, where the existence of two different amorphous forms, high-density amorphous (HDA) and low-density amorphous (LDA) ice was experimentally known since

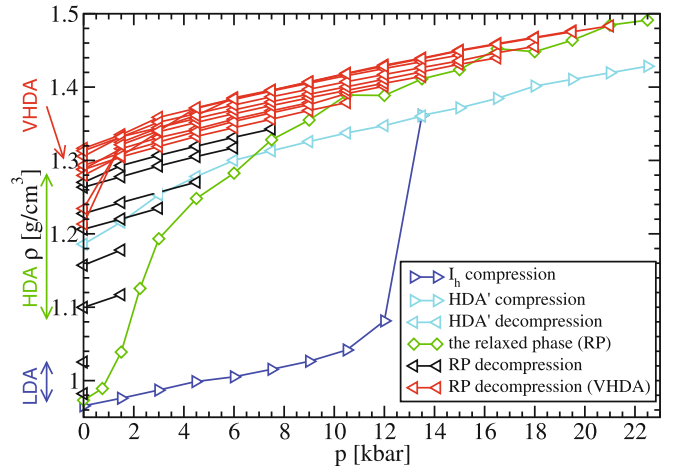


Fig. 5. Density vs. pressure dependence at $T = 80$ K for the various amorphous phases of ice during compression/decompression. The triangles point in the direction of pressure change, the lines are just a guide for the eye. After reference [72]. Reprinted with permission from [72] Copyright 2005, American Institute of Physics.

long time [64–66]. The process of pressure-induced amorphization of hexagonal ice I_h was also studied by simulations [67,68]. The observed polyamorphism has been suggested to be an indirect manifestation of the hypothetical second critical point located in the metastable deeply supercooled regime, as proposed in reference [69]. Because of the high importance of water there has been a large experimental and theoretical activity in this field. In reference [70] a third form of amorphous ice was found experimentally and called very high-density amorphous (VHDA) ice. This finding motivated new experimental research as well as new simulations, both aiming at deciding whether the existence of three kinds of amorphous ice is still compatible with the scenario of the second critical point.

As an example of these simulational studies we mention here the references [71,72], where the evolution of structure of amorphous ice upon compression and decompression combined with thermal treatment was studied by the Parrinello-Raman MD using the classical TIP4P model of water [73]. Because structural changes in amorphous ice take place on slow time scales, it was necessary to perform long simulations and for this reason a relatively small system consisting of 360 H₂O molecules was chosen. The evolution of density is summarized in Figure 5. In order to characterize the structural evolution besides the pair correlation function also the statistics of hydrogen-bonded rings was analyzed which provides information about medium-range order. The findings were compatible with the existence of two megabasins, LDA and HDA. However, within the HDA megabasin the structure undergoes a pronounced evolution from the onset of HDA regime at pressure of about 2 kbar until entering the VHDA regime at about 10 kbar. The VHDA form was found to be a limiting form of HDA and therefore its existence does not seem to contradict the scenario of the

second critical point. Because of the small size of the system as well as difficulties in equilibration it was not possible to decide whether the LDA/HDA transition is a real first-order transition or just a crossover. Other simulations of amorphous ices focused on the structure of the VHDA ice were presented in references [74–76]. We also mention a comparison of experiments and simulations in reference [77] as well as an exhaustive review focused on the same topic in reference [78].

6 Simulations of finite objects under pressure

Due to the advent of nanotechnologies it became possible to prepare small clusters and nanocrystals in controlled way. When the small objects are dissolved in liquid, one can study them under pressure and in this way investigate pressure-induced structural transitions on small scales. It is often stated that “small is different” and one can expect that the transitions in nanoobjects may not be simple analogues of the ones observed in bulk systems. While in the extreme limit of very small clusters the structural transformations correspond to molecular isomerization, the intermediate regime is particularly interesting. Here, on the one hand, the surface contribution to the free energy becomes relevant and on the other hand, when the object becomes smaller than the size of the nucleation region, the transition mechanism might deviate from the one operative in the bulk. These effects were studied in a series of experiments [79–86]. Other examples include, e.g., experiments on carbon nanotubes under pressure [87].

Clearly, also in this field computer simulations are likely to be highly useful. The simulation methods discussed in the previous sections, based on the use of periodic box and rescaling of the particle coordinates, however, cannot be directly applied to this case. The objects under study are finite objects with essentially arbitrary shape, and lack translational invariance and periodicity. In order to study this class of systems it is necessary to develop a suitable simulational technique. Here we briefly review several approaches that have been proposed in the last decade or so.

The first approach was based on mimicking the experiment, where external pressure is applied on nanoobjects dissolved in suitable liquid by compressing the liquid. In such setup, the liquid acts as pressure-transmitting medium. In computer simulation the real liquid may be replaced by artificial model liquid, which can be described in a simple way, e.g. by purely repulsive classical interactions between the liquid particles. The liquid particles interact with nanoobject particles via short-range forces, exerting corresponding normal forces on the surface of the nanoobject. This approach was first applied in reference [15], where soft-sphere classical liquid with interparticle interactions decaying as R^{-12} was used as pressure-transmitting medium. The technique was applied to ab initio study of small silicon clusters, $\text{Si}_{35}\text{H}_{36}$ in reference [15] and $\text{Si}_{71}\text{H}_{60}$ in reference [88], described by the Car-Parrinello MD [20]. Upon compression of the clusters a transition to amorphous state was observed and

upon decompression a transition to structurally different amorphous state was observed. In reference [89] these transitions were interpreted as manifestation of polyamorphism in small silicon clusters. In reference [90] the same simulation technique was applied to a medium-sized silicon nanocrystal Si_{705} described by the tight-binding MD, with similar results. We note here that according to reference [86] polyamorphism in nanocrystalline objects might be actually widespread and could exist even in materials which in bulk are poor glass formers. Variants of the pressure-transmitting liquid approach were applied in references [91,92] where different interparticle potentials were used for the liquid. Conceptually similar approach was described in reference [17] where ideal gas was used as pressure-transmitting medium. The latter algorithm was also combined with transition path sampling and applied to the study of mechanisms of nucleation and growth in pressure-induced structural transformations in CdSe nanocrystals [93,94].

It is also possible to apply the external force directly to the nanoobject, as proposed in reference [95], where Brownian forces act on the surface atoms. Another possibility was explored in reference [96], where the surface of the nanoobject is identified by calculating the minimal convex polyhedron enclosing all atoms using the quickhull algorithm [97]. This approach was applied to the simulation of carbon nanotube under pressure. In Figure 6 the evolution of shape of carbon nanotube upon increasing external pressure is shown. It is seen that the cross section undergoes at certain pressure a transition from ellipsoidal to peanut shape.

Another class of possible approaches is in spirit closer to the Parrinello-Rahman MD technique. The starting point is, similarly to equation (1), an addition of a PV term to the potential energy of the system. It can be shown that one can then derive equations of motion of the particles where the forces include a contribution from the external pressure P and the average internal pressure in the system is equal to the external pressure P [16,98]. Within this approach there is no need for the pressure-transmitting medium or external force applied to the surface. The main problem, however, is how to calculate the volume of the system V . Since the system is not periodically replicated, the volume is not defined by the simulation supercell but has to be defined as some suitable function of the coordinates of the atoms. Clearly, for relatively small systems there is no unique way of calculating the volume. For systems described by density-functional theory it is possible to calculate the volume of the system in a well-defined way using the electronic density isosurface and such approach was suggested in reference [99]. For systems where electronic density is not available various approximations were proposed and several of them are reviewed in reference [16]. Here we mention the approximation of the volume by that of a simple body with regular shape the size of which is determined by calculating the respective radii of gyration from the inertia tensor of the system. This approach was originally proposed in reference [100] for objects of ellipsoidal shape and later applied in reference [16] to the MD simulation of C_{60} fullerene.

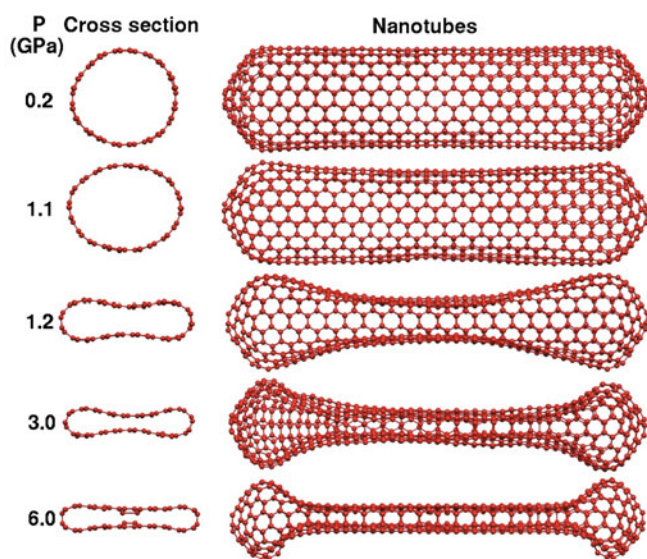


Fig. 6. Snapshots at different pressures of a (10, 10) armchair carbon nanotube, 60 Å long, consisting of 1020 atoms and at a temperature of 50 K. In (a) we obtain a cylindrical structure by applying 0.2 GPa, in (b) the shape is ellipsoidal at 1.1 GPa and for (c), (d) and (e) a peanut-shape structure is obtained for 1.2, 3.0 and 6.0 GPa, respectively. As the pressure is increased, the nanotube has less freedom to vibrate along the radial direction, and at some specific pressure, the system prefers to bend. Adapted from reference [96].

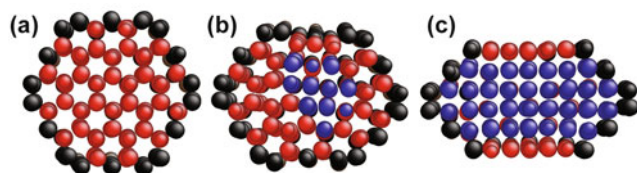


Fig. 7. Snapshots of a cross-section of the $\text{Cd}_{432}\text{Se}_{432}$ nanorod during the transition from HS to RS. (a) at $t = 500$ ps; (b) at $t = 523$ ps; (c) $t = 528$ ps. The atoms are colored according to the number of nearest neighbors within a distance of 3.5 Å, with black indicating four, red five, and blue six nearest neighbors. After reference [98] – reproduced by permission of the PCCP owner Societies.

More recently, this technique was generalized to cylindrical and cuboidal nano-objects [98]. As an example of the application of this method to a cylindrical nanobject a $\text{Cd}_{432}\text{Se}_{432}$ nanorod described by a classical potential was studied under pressure, starting from the wurtzite structure. Figure 7 shows the second stage of the transition where the intermediate fivefold coordinated honeycomb-stacked (HS) structure transforms into the final six-fold coordinated rocksalt (RS) structure.

7 Conclusions and outlook

In this review we discussed a range of topics related to computer simulations of pressure-induced structural transformations in various kinds of condensed matter sys-

tems, including both bulk and finite systems with crystalline as well as amorphous structure. A straightforward approach based on plain constant-pressure MD encounters here a severe time-scale problem. During the last decade this difficulty motivated the application of advanced techniques developed for study of activated processes, such as metadynamics and transition path sampling. These approaches can also be combined with the techniques enabling the simulation of finite objects under pressure. The applicability of these new algorithms has been already successfully demonstrated on a number of systems. It is thus safe to say that computer simulations nowadays provide a solid route to study structural transformations, and are capable not only to complement the experiment, but have also a predictive power, especially when *ab initio* techniques are used. However, there is still a long way towards fully realistic simulations. Further improvement of simulation algorithms in this field is likely to address the problem of realistic simulation of nucleation and growth processes, including the role of structural defects in bulk systems.

The author is grateful to C. Molteni, S. Leoni, D. Donadio, J. Sun and A.H. Romero for kindly agreeing to use their figures. The author has been supported by the Slovak Research and Development Agency under Contracts No. APVV-0442-07 and No. VVCE-0058-07.

References

1. J. Schön, M. Jansen, *Angew. Chem. Int. Ed.* **35**, 1287 (1996)
2. A. Oganov, C. Glass, *J. Chem. Phys.* **124**, 244704 (2006)
3. C.J. Pickard, R.J. Needs, *Phys. Rev. Lett.* **97**, 045504 (2006)
4. P.F. Mcmillan, *Nat. Mater.* **1**, 19 (2002)
5. G.R. Desiraju, *Nat. Mater.* **1**, 77 (2002)
6. R.J. Hemley, H.K. Mao, *Mineralogical Magazine* **66**, 791 (2002)
7. D.K. Bradley, J.H. Eggert, R.F. Smith, S.T. Prisbrey, D.G. Hicks, D.G. Braun, J. Biener, A.V. Hamza, R.E. Rudd, G.W. Collins, *Phys. Rev. Lett.* **102**, 075503 (2009)
8. M. Parrinello, A. Rahman, *Phys. Rev. Lett.* **45**, 1196 (1980)
9. R. Martoňák, A. Laio, M. Parrinello, *Phys. Rev. Lett.* **90**, 075503 (2003)
10. A. Laio, M. Parrinello, *Proc. Natl. Acad. Sci. USA* **99**, 12562 (2002)
11. C. Dellago, P. Bolhuis, F. Csajka, D. Chandler, *J. Chem. Phys.* **108**, 1964 (1998)
12. D. Zahn, S. Leoni, *Phys. Rev. Lett.* **92**, 250201 (2004)
13. D. Zahn, S. Leoni, *Z. Kristallogr.* **219**, 345 (2004)
14. S. Leoni, R. Ramlau, K. Meier, M. Schmidt, U. Schwarz, *PNAS* **105**, 19612 (2008)
15. R. Martoňák, C. Molteni, M. Parrinello, *Phys. Rev. Lett.* **84**, 682 (2000)
16. S. Baltazar, A. Romero, J.L. Rodríguez-López, H. Terrones, R. Martoňák, *Comput. Mater. Sci.* **37**, 526 (2006)
17. M. Gruenwald, C. Dellago, *Mol. Phys.* **104**, 3709 (2006)
18. H.C. Andersen, *J. Chem. Phys.* **72**, 2384 (1980)

19. W.G. Hoover, Phys. Rev. A **31**, 1695 (1985)
20. R. Car, M. Parrinello, Phys. Rev. Lett. **55**, 2471 (1985)
21. M. Parrinello, A. Rahman, J. Appl. Phys. **52**, 7182 (1981)
22. S. Nosé, M.L. Klein, Mol. Phys. **50**, 1055 (1983)
23. S. Nosé, Mol. Phys. **52**, 255 (1984)
24. S. Melchionna, G. Ciccotti, B. Holian, Mol. Phys. **78**, 533 (1993)
25. R.M. Wentzcovitch, Phys. Rev. B **44**, 2358 (1991)
26. G. Martyna, D. Tobias, M. Klein, J. Chem. Phys. **101**, 4177 (1994)
27. G. Martyna, M. Klein, M. Tuckerman, J. Chem. Phys. **97**, 2635 (1992)
28. I. Souza, J.L. Martins, Phys. Rev. B **55**, 8733 (1997)
29. H.J.C. Berendsen, J.P.M. Postma, W.F. van Gunsteren, A. DiNola, J.R. Haak, J. Chem. Phys. **81**, 3684 (1984)
30. G. Bussi, D. Donadio, M. Parrinello, J. Chem. Phys. **126**, 014101 (2007)
31. G. Bussi, T. Zykova-Timan, M. Parrinello, J. Chem. Phys. **130**, 074101 (2009)
32. P. Focher, G.L. Chiarotti, M. Bernasconi, E. Tosatti, M. Parrinello, Europhys. Lett. **26**, 345 (1994)
33. R. Martoňák, A. Laio, M. Bernasconi, C. Ceriani, P. Raiteri, F. Zipoli, M. Parrinello, Z. Kristallogr. **220**, 489 (2005)
34. A.F. Voter, Phys. Rev. Lett. **78**, 3908 (1997)
35. H. Grubmüller, Phys. Rev. E **52**, 2893 (1995)
36. T. Huber, A.E. Torda, W.F. van Gunsteren, J. Comput.-Aided Mol. Des. **8**, 695 (1994)
37. E. Carter, G. Ciccotti, J. Hynes, R. Kapral, Chem. Phys. Lett. **156**, 472 (1989)
38. M. Sprik, G. Ciccotti, J. Chem. Phys. **109**, 7737 (1998)
39. A. Laio, M. Parrinello, Lect. Notes Phys. **703**, 315 (2006)
40. A. Laio, F.L. Gervasio, Rep. Prog. Phys. **71**, 126601 (2008)
41. R. Martoňák, A.R. Oganov, C.W. Glass, Phase Transitions **80**, 277 (2007)
42. P. Raiteri, R. Martoňák, M. Parrinello, Angew. Chem. Int. Ed. **44**, 3769 (2005)
43. C. Ceriani, A. Laio, E. Fois, A. Gamba, R. Martoňák, M. Parrinello, Phys. Rev. B **70**, 113403 (2004)
44. A.R. Oganov, R. Martoňák, A. Laio, P. Raiteri, M. Parrinello, Nature **438**, 1142 (2005)
45. T. Ishikawa, H. Nagara, K. Kusakabe, N. Suzuki, Phys. Rev. Lett. **96**, 095502 (2006)
46. M. Pagliai, M. Iannuzzi, G. Cardini, M. Parrinello, V. Schettino, Chem. Phys. Chem. **7**, 141 (2006)
47. R. Martoňák, D. Donadio, A.R. Oganov, M. Parrinello, Nat. Mater. **5**, 623 (2006)
48. R. Martoňák, D. Donadio, A.R. Oganov, M. Parrinello, Phys. Rev. B **76**, 014120 (2007)
49. R. Martoňák, in *Modern methods of crystal structure prediction*, edited by A.R. Oganov (Wiley-VCH, Berlin, 2011)
50. J. Sun, D.D. Klug, R. Martoňák, J. Chem. Phys. **130**, 194512 (2009)
51. D. Donadio, R. Martoňák, P. Raiteri, M. Parrinello, Phys. Rev. Lett. **100**, 165502 (2008)
52. J. Behler, R. Martoňák, D. Donadio, M. Parrinello, Phys. Rev. Lett. **100**, 185501 (2008)
53. J. Behler, R. Martoňák, D. Donadio, M. Parrinello, Physica Status Solidi (b) **245**, 2618 (2008)
54. J. Sun, D.D. Klug, R. Martoňák, J.A. Montoya, M.S. Lee, S. Scandolo, E. Tosatti, PNAS **106**, 6077 (2009)
55. Y. Yao, D.D. Klug, J. Sun, R. Martoňák, Phys. Rev. Lett. **103**, 055503 (2009)
56. S. Jahn, R. Martoňák, Phys. Chem. Minerals **35**, 17 (2008)
57. S. Jahn, R. Martoňák, Am. Mineral. **94**, 950 (2009)
58. C. Bealing, R. Martoňák, C. Molteni, J. Chem. Phys. **130**, 124712 (2009)
59. L.S. Dubrovinsky, N.A. Dubrovinskaja, S.K. Saxena, F. Tutti, S. Rekh, T.L. Bihan, G. Shen, J. Hu, Chem. Phys. Lett. **333**, 264 (2001)
60. S.R. Shieh, T.S. Duffy, G. Shen, Earth and Planetary Science Letters **235**, 273 (2005)
61. M. Santoro, F.A. Gorelli, R. Bini, G. Ruocco, S. Scandolo, W.A. Crichton, Nature **441**, 857 (2006)
62. T. Kume, Y. Ohya, M. Nagata, S. Sasaki, H. Shimizu, J. Appl. Phys. **102**, 53501 (2007)
63. S.E. Boulfelfel, D. Zahn, Y. Grin, S. Leoni, Phys. Rev. Lett. **99**, 125505 (2007)
64. O. Mishima, L.D. Calvert, E. Whalley, Nature (London) **310**, 393 (1984)
65. O. Mishima, L.D. Calvert, E. Whalley, Nature (London) **314**, 76 (1985)
66. O. Mishima, J. Chem. Phys. **100**, 5910 (1994)
67. J.S. Tse, M.L. Klein, Phys. Rev. Lett. **58**, 1672 (1987)
68. I. Okabe, H. Tanaka, K. Nakanishi, Phys. Rev. E **53**, 2638 (1996)
69. P.H. Poole, F. Sciortino, U. Essmann, H.E. Stanley, Nature **360**, 324 (1992)
70. T. Loerting, C. Salzmann, I. Kohl, E. Mayer, A. Hallbrucker, Phys. Chem. Chem. Phys. **3**, 5355 (2001)
71. R. Martoňák, D. Donadio, M. Parrinello, Phys. Rev. Lett. **92**, 225702 (2004)
72. R. Martoňák, D. Donadio, M. Parrinello, J. Chem. Phys. **122**, 134501 (2005)
73. W.L. Jorgensen, J. Chandrasekhar, J.D. Madura, R.W. Impey, M.L. Klein, J. Chem. Phys. **79**, 926 (1983)
74. B. Guillot, Y. Guissani, J. Chem. Phys. **119**, 11740 (2003)
75. I. Brovchenko, A. Geiger, A. Oleinikova, J. Chem. Phys. **118**, 9473 (2003)
76. A.M. Saitta, T. Strässle, G. Rousse, G. Hamel, S. Klotz, R.J. Nelmes, J.S. Loveday, J. Chem. Phys. **121**, 8430 (2004)
77. I. Brovchenko, A. Oleinikova, J. Chem. Phys. **124**, 164505 (2006)
78. T. Loerting, N. Giovambattista, J. Phys.: Condens. Matter **18**, R919 (2006)
79. S.H. Tolbert, A.P. Alivisatos, J. Chem. Phys. **102**, 4642 (1995)
80. S.H. Tolbert, A.P. Alivisatos, Science **265**, 373 (1994)
81. S.H. Tolbert, A.P. Alivisatos, Annu. Rev. Phys. Chem. **46**, 595 (1995)
82. S.H. Tolbert, A.B. Herhold, L.E. Brus, A.P. Alivisatos, Phys. Rev. Lett. **76**, 4384 (1996)
83. J.N. Wickham, A.B. Herhold, A.P. Alivisatos, Phys. Rev. Lett. **84**, 923 (2000)
84. C.C. Chen, A.B. Herhold, C.S. Johnson, A.P. Alivisatos, Science **276**, 398 (1997)

85. K. Jacobs, D. Zaziski, E.C. Scher, A.B. Herhold, A.P. Alivisatos, *Science* **293**, 1803 (2001)
86. V. Swamy, A. Kuznetsov, L.S. Dubrovinsky, P.F. McMillan, V.B. Prakapenka, G. Shen, B.C. Muddle, *Phys. Rev. Lett.* **96**, 135702 (2006)
87. J. Tang, L.C. Qin, T. Sasaki, M. Yudasaka, A. Matsushita, S. Iijima, *Phys. Rev. Lett.* **85**, 1887 (2000)
88. C. Molteni, R. Martoňák, M. Parrinello, *J. Chem. Phys.* **114**, 5358 (2001)
89. C. Molteni, R. Martoňák, *Chem. Phys. Chem.* **6**, 1765 (2005)
90. R. Martoňák, L. Colombo, C. Molteni, M. Parrinello, *J. Chem. Phys.* **117**, 11329 (2002)
91. S. Kodiyalam, R.K. Kalia, H. Kikuchi, A. Nakano, F. Shimojo, P. Vashishta, *Phys. Rev. Lett.* **86**, 55 (2001)
92. B.J. Morgan, P.A. Madden, *Nano Lett.* **4**, 1581 (2004)
93. M. Gruenwald, C. Dellago, *Nano Lett.* **9**, 2099 (2009)
94. M. Gruenwald, C. Dellago, *J. Chem. Phys.* **131**, 164116 (2009)
95. J. Kohanoff, A. Caro, M.W. Finnis, *Chem. Phys. Chem.* **6**, 1848 (2005)
96. S.E. Baltazar, A.H. Romero, J.L. Rodríguez-López, R. Martoňák, *J. Phys.: Condens. Matter* **18**, 9119 (2006)
97. C.B. Barber, D.P. Dobkin, H. Huhdanpaa, *ACM Trans. Math. Softw.* **22**, 469 (1996)
98. C. Bealing, G. Fugallo, R. Martoňák, C. Molteni, *Phys. Chem. Chem. Phys.* **12**, 8542 (2010)
99. M. Cococcioni, F. Mauri, G. Ceder, N. Marzari, *Phys. Rev. Lett.* **94**, 145501 (2005)
100. D.Y. Sun, X.G. Gong, *Phys. Rev. B* **57**, 4730 (1998)